DALTON

Nickel(II) N_2O_2 Schiff-base complexes incorporating pyrazole: syntheses, characterization and acidity of the metal centre towards co-ordinating solvents †

Agnete la Cour,*[a] Matthias Findeisen,[b] Rita Hazell,[c] Lothar Hennig,[b] Carl Erik Olsen[d] and Ole Simonsen[a]

[a] *Department of Chemistry, Odense University, DK-5230, Odense M, Denmark*
[b] *Department of Organic Chemistry, Leipzig University, D-04103 Leipzig, Germany*
[c] *Department of Chemistry, Aarhus University, DK-8000 Århus C, Denmark*
[d] *The Royal Veterinary and Agricultural University, DK-1871 Frederiksberg C, Denmark*

A series of four-co-ordinate nickel(II) complexes have been prepared containing a tetradentate N_2O_2 aldimine or ketoimine Schiff-base ligand formed by condensation of 4-formyl-5-hydroxy- or 4-benzoyl-5-hydroxy-pyrazoles with aliphatic diamines containing two or three carbon atoms (n = 2 or 3). In non-donor solvents the low-spin (S = 0) state is favoured. The complexes with n = 2 are fully diamagnetic; the spin-equilibrium process (S = 0) $\rightleftharpoons$ (S = 1) is, however, induced when n = 3. The crystal structure has been determined of {*N*,*N*′-bis[(5-hydroxy-1,3-diphenylpyrazolyl)phenylmethylene]propane-1,3-diaminato}nickel(II) **1a** which has a flattened tetrahedral geometry, and the spin-equilibrium process has been investigated for selected complexes by spectroscopic methods [ΔH 16–21 kJ mol^{-1}, ΔS 2–22 J K^{-1} mol^{-1}, and ΔG(50 °C) 14–19 kJ mol^{-1}]. The four-co-ordinate complexes reversibly increase their co-ordination numbers in donor solvents (all) or by molecular association in non-donor solvents (the aldimine complexes only). Solid six-co-ordinate products from the reactions with dimethylsulfoxide (dmso), pyridine and water have been isolated, and the crystal structures determined of the product (**1b**) from the reaction of **1a** with dmso and of that (**3b**) from the reaction of {*N*,*N*′-bis[(5-hydroxy-1,3-diphenylpyrazolyl)(*p*-tolyl)methylene]propane-1,3-diaminato}nickel(II) with dmso. Complexes **1b** and **3b** have *trans* distorted-octahedral geometries with O-bound dmso molecules in axial positions. The adduct formation with dmso [$-\Delta H$ 10–27 kJ mol^{-1}, $-\Delta S$ 57–107 J K^{-1} mol^{-1}, ΔG(25 °C) 0.9–7.0 kJ mol^{-1}] and with pyridine [ΔG(25 °C) −19 kJ mol^{-1}] has been investigated for selected complexes by spectroscopic methods. Angular overlap model ligand-field parameters have been derived from the electronic absorption spectra.

It is well known that Ni^{II} four-co-ordinated with oxygen donors or a mixed nitrogen–oxygen donor set tends to increase its co-ordination number to five or six by self-association[1] or by addition of Lewis bases.[1a–c,f,2] Also, four-co-ordinate Ni^{II} will often be in spin equilibrium,[1b,c,3] see equations (1)–(3) where L

$$\text{NiL } (S = 0) \overset{K_1}{\rightleftharpoons} \text{NiL } (S = 1); \quad K_1 = N_{hs}/N_{ls} = N_{hs}/(1 - N_{hs}) \quad (1)$$

$$x\text{NiL} \overset{\beta'}{\rightleftharpoons} (\text{NiL})_x;\ \beta' = [\text{oligomer}]/[\text{monomer}]^x \quad (2)$$

$$\text{NiL} \overset{B,K_2}{\rightleftharpoons} \text{NiL(B)} \overset{B,K_3}{\rightleftharpoons} \text{NiLB}_2;\ \beta = K_2K_3 \quad (3)$$

$$K_2 = [\text{NiL(B)}]/[\text{NiL}][\text{B}],\ K_3 = [\text{NiLB}_2]/[\text{NiL(B)}][\text{B}]$$

is a N_2O_2 ligand, N_{hs} and N_{ls} are the mole fractions of the high- and low-spin forms, and B is a Lewis base.

These processes have been extensively studied with bi- and tetra-dentate Schiff bases formed by condensation of β-diketones, salicylaldehydes,[4] or *o*-hydroxybenzophenones[1e,2b] with aliphatic or aromatic mono- or di-amines. The preference for the low-spin (S = 0) state is strong for the four-co-ordinate chelate. The normally endothermic spin-equilibrium process (1) is induced by bidentate compounds with bulky substituents[1b,2c,3b–f] and tetradentate ligands containing biphenyl or naphthyl linkages,[3a] but not by tetradentate ones containing aliphatic linkages (n = 2–12).[1d,e] The tendency to increase the co-ordination number by molecular association in the solid state and in non-donor solvents [equation (2)] can be reduced or totally prevented by the introduction of sterically demanding substituents[1a,e] thus facilitating investigation of the four-co-ordinate monomers.[1e] The formation of paramagnetic compounds by molecular self-association or by adduct formation with donor solvents [equation (3)] is usually an exothermic process.[1a,2a,b,d]

In this work we have prepared a series of nickel(II) complexes with tetradentate N_2O_2 Schiff-base ligands based on 4-formyl-5-hydroxy- or 4-benzoyl-5-hydroxy-pyrazoles and aliphatic diamines (n = 2 or 3). A general characterization is given of these new systems, and relations between the properties of the four-co-ordinate chelate and the acidity of the metal centre are discussed.

Results and Discussion

Syntheses and identification

The complexes were identified from the satisfactory elemental analyses and from the electron-impact mass spectra. The parent four-co-ordinate complexes are denoted by an arabic number followed by **a**, the six-co-ordinate adducts by the same number followed by **b** (dimethyl sulfoxide, dmso), **c** (pyridine), or **d** (water). The four-co-ordinate complex **7a** is not stable in solution in contrast with the solvated complex; the free pro-ligand is observed in the ^{1}H NMR spectrum in $CDCl_3$ but not

† *Supplementary data available* (No. SUP 57154, 12 pp.): equilibrium and NMR data and electronic spectra. See Instructions for Authors, *J. Chem. Soc., Dalton Trans.*, 1996, Issue 1.

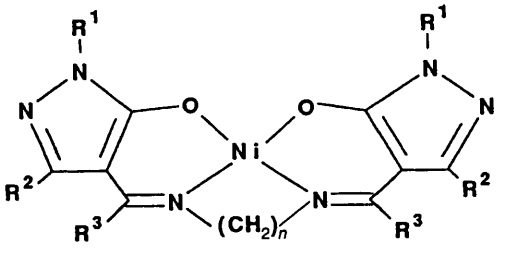

	n	R^1	R^2	R^3
1a	3	Ph	Ph	Ph
2a	3	Ph	Ph	*p*-ClC_6H_4
3a	3	Ph	Ph	*p*-MeC_6H_4
4a	3	Ph	Ph	*p*-$O_2NC_6H_4$
5a	3	Ph	Me	Ph
6a	3	Ph	Me	*p*-ClC_6H_4
7a	3	Ph	Me	*p*-MeC_6H_4
8a	2	Ph	Me	Ph
9a	3	Me	Ph	Ph
10a	2	Me	Ph	Ph
11a	3	Ph	Ph	H
12a	3	Ph	Me	H
13a	2	Ph	Me	H
14a*	2	Ph	Me	H

* The chain is $CHMeCH_2$

Table 1 Yields and analytical data for the complexes

Complex	Yield[a] (%)	Analysis (%)[b] C	H	N	EI mass spectrum, *m/z*[c]
1a·0.5$CHCl_3$	84.3	68.6	4.50	10.1	774
	(86.7)	(68.3)	(4.40)	(10.05)	
1b·2dmso		66.25	5.20	9.20	
		(65.75)	(5.20)	(9.00)	
1c·2C_5H_5N		72.75	5.05	11.35	
		(73.3)	(4.95)	(12.00)	
2a	88.7	66.95	4.15	10.05	844[d]
	(93.1)	(66.85)	(4.05)	(9.95)	
3a	84.6	72.6	5.00	10.35	802
	(93.0)	(73.25)	(5.00)	(10.45)	
4a	72.3	65.1	3.95	13.1	864
	(93.6)	(65.2)	(3.95)	(12.95)	
5a·0.1$CHCl_3$	77.3	67.65	4.85	12.7	650
	(92.1)	(67.2)	(4.90)	(12.65)	
6a	67.8	61.25	4.15	11.7	718
	(56.2)	(61.7)	(4.20)	(11.65)	
6b·2dmso		56.7	4.60	10.55	
		(56.2)	(4.85)	(9.60)	
7a	41.8	68.5	5.30	12.4	678
	(81.6)	(68.95)	(5.35)	(12.35)	
8a	93.5	67.7	4.70	13.3	636
	(80.6)	(67.85)	(4.75)	(13.2)	
9a·1.25$CHCl_3$	55.2	57.6	4.15	10.4	650
	(90.9)	(57.35)	(4.20)	(10.5)	
10a	92.9	67.65	4.65	13.2	636
	(48.5)	(67.85)	(4.75)	(13.2)	
11a·$CHCl_3$	24.5	58.45	4.05	11.4	622
	(27.5)	(58.2)	(3.95)	(11.3)	
12d·2H_2O[e]	85.8	56.25	5.20	15.7	498
	(95.7)	(56.1)	(5.25)	(15.7)	
13a	90.7	58.55	4.50	17.4	484
	(93.2)	(59.4)	(4.55)	(17.3)	
14a	74.2	60.25	4.90	16.65	498
	(≈2)	(60.15)	(4.85)	(16.85)	

[a] Yields of pro-ligands in parentheses. [b] Calculated values in parentheses. [c] Crystal solvent or axial ligands are not included in the molecular ion, M^+. [d] $M^+ + 2$. [e] Data from preparation method 1.

in $(CD_3)_2SO$. A slight tendency to lose ligand is also observed for **3a**. Solid **12a** takes up water, probably as axial ligands: the process can be followed by the colour change; the four-co-ordinate complex is red, the water adduct **12d** is light green. The elemental analysis is consistent with two bound water

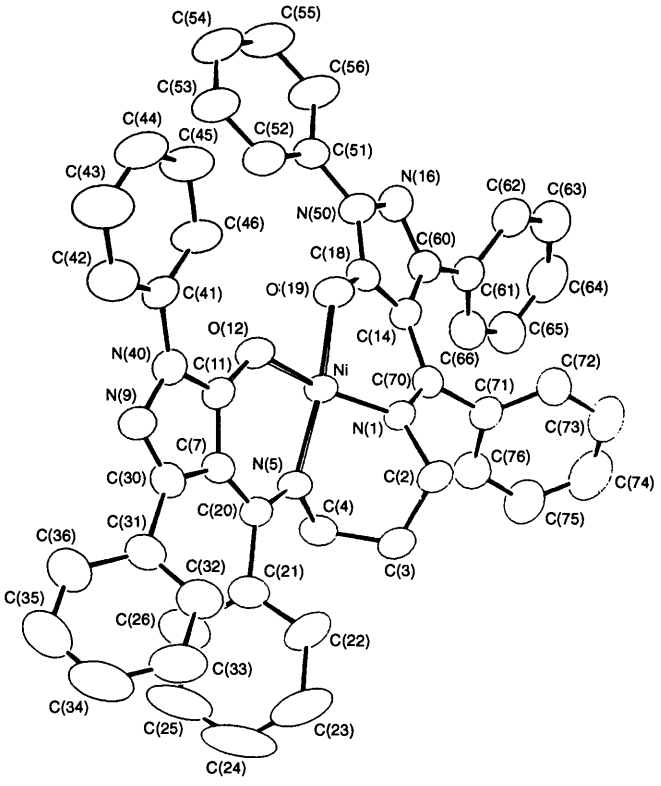

Fig. 1 Molecular structure of complex **1a**

molecules. When heated, the water ligands are lost. The complex returns, however, to the green form within a few minutes. The six-co-ordinate pyridine adduct **1c** and the dmso adducts **1b**, **3b** and **6b** were also isolated as analytically pure solids.

Crytal structures

Selected bond distances and angles are given in Table 2.

Complex 1a. The molecular structure is shown in Fig. 1. It contains discrete molecules without significant intermolecular interactions, the shortest distances to donor atoms in a neighbouring molecule being 5.896(8) [Ni···N(1)] and 6.360 Å [Ni···O(19)], and the shortest Ni···Ni distance is 5.312(2) Å.

Conjugation between the phenyl substituents and the pyrazolyl and chelate rings is indicated by selected torsion angles: Ph^1 C(11)–N(40)–C(41)–C(46) 7(2), C(18)–N(50)–C(51)–C(52) −178(1); Ph^2 C(7)–C(30)–C(31)–C(36) −129(1), C(14)–C(60)–C(61)–C(66) 42(2); Ph^3 C(7)–C(20)–C(21)–C(26) 73(1), C(14)–C(70)–C(71)–C(76) −112(1)°. A considerable deviation from 90° is seen, greatest for Ph^1, least for Ph^3. Disorder of the incorporated crystal chloroform lowered the quality of the data set, and detailed comparison of bond distances is not appropriate. The conjugation is, however, weakly reflected in the bond lengths N(40)–C(41) and N(50)–C(51) [1.44(1) and 1.41(1) Å] compared with the N–C distances of the aliphatic chain [1.46(1), 1.45(1) Å]. The C–C distances to phenyl are not significantly different from the C–C distances of the chain (1.50 Å).

The delocalization of electron density in the chelate rings is reflected in the bond lengths, and is comparable to that in tetradentate N_2O_2 Schiff-base complexes of Ni^{II} containing aromatic carbon cycles[5] (*n* = 2 or 3).

The surroundings of the nickel atom are pseudo-tetrahedral and more distorted from square planar than in comparable systems (*n* = 3) based on aromatic carbon cycles.[5a,b] The angle θ between the planes N(1)–Ni–O(19) and O(12)–Ni–N(5) is 12.7°. The weakly umbrella-shaped complex *N*,*N*′-

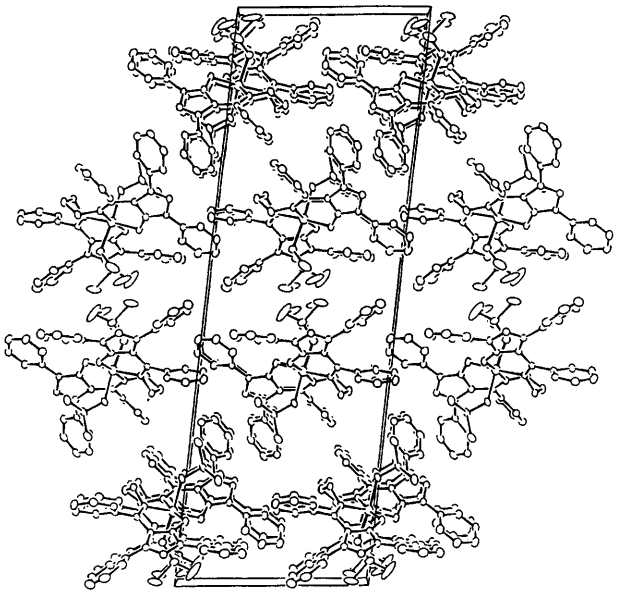

Fig. 2 Packing diagram for complex **1b**

[bis(2-hydroxy-1-naphthylmethylene)propane-1,3-diaminato]-nickel(II) [5a] is almost planar, θ = 2°. In the complex [*N*,*N*′-bis(salicylidene)propane-1,3-diaminato]nickel, [Ni(salpd)],[5b] θ is 9°, and again the distortion is a fold rather than a tetrahedral twist. The metal–ligand bonds in **1a** are as in the two comparable systems [5a,b] and longer than in the analogous $n = 2$ complexes,[5c–e] *e.g.* in [*N*,*N*′-bis(salicylidene)ethane-1,2-diaminato]nickel, [Ni(salen)] M–O 1.850(2), 1.855(2) Å and M–N 1.853(2), 1.843(2) Å.[5e]

Complex 1b. The packing diagram is presented in Fig. 2. The numbering is as for complex **3b** (see Fig. 3). Anomalously high thermal motions for atoms C(15) and C(17) are ascribed to the disorder of one dmso ligand. The structure contains discrete molecules without significant intermolecular interactions. The observed stacking is due to packing forces alone.

The in-plane M–L bond distances fall within the range found for in-plane Ni–N and Ni–O bonds in similar axially distorted (pseudo)octahedral complexes.[6] They are longer than in the parent complex **1a** and shorter than the axial M–O (dmso) bonds. The bond distances in the chelate rings are as in the parent complex; the delocalization of electron density in the rings does not seem to be influenced by the adduct formation.

As in the four-co-ordinate parent complex, the torsion angles indicate that the phenyl groups are involved in conjugation with the chelate and pyrazolyl rings: Ph^1 C(11)–N(40)–C(41)–C(46) 36.2(6), C(18)–N(50)–C(51)–C(52) − 157.2(4); Ph^2 C(7)–C(30)–C(31)–C(36) 155.0(4), C(14)–C(60)–C(61)–C(66) −36.4(7); Ph^3 C(7)–C(20)–C(21)–C(26) − 52.6(5), C(14)–C(70)–C(71)–C(76) 126.9(4)°. Considerable deviations from 90° are seen, more so for Ph^2 and Ph^3 less for Ph^1 than in the four-co-ordinate complex. The conjugation is reflected in the N–C and C–C distances to phenyl, N–C(R^1) = 1.401(5), 1.419(5), C–C(R^2) 1.474(6), 1.457(6), C–C(R^3) 1.498(6), 1.496(5) Å. They are significantly shorter than the normal [7] bond lengths of the aliphatic chain, N–C 1.458(6), 1.457(5) Å, C–C 1.542(6), 1.533(6) Å, and fall within the range for sp^2–sp^2 N–C and C–C single bonds in conjugated systems [7] [N–C 1.431(20)–1.468(14), C–C 1.487(7) Å for aromatic carbon].

Complex 3b. The molecular structure is shown in Fig. 3. The minor component of one disordered dmso ligand has been omitted for simplicity. The co-ordination in this complex is similar to that in **1b**. The M–L distances are, however, significantly longer, and the puckering of the six-membered ring is different. The ligand has approximate mirror symmetry

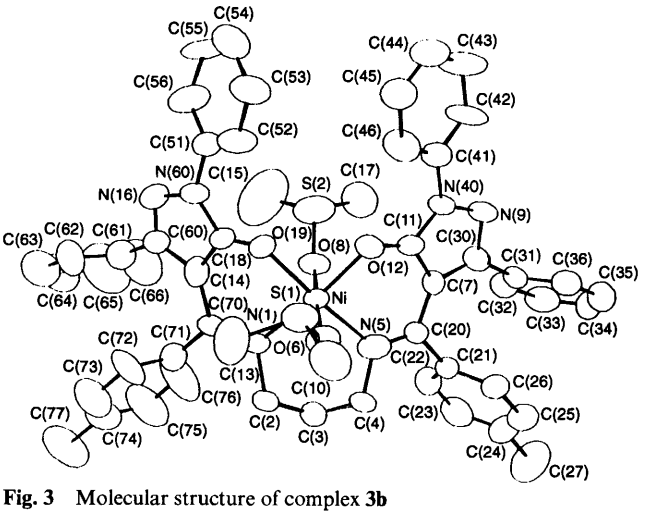

Fig. 3 Molecular structure of complex **3b**

Table 2 Selected interatomic distances (Å) and angles (°) for complexes **1a**, **1b** and **3b**

	1a	**1b**	**3b**
Ni–N(1)	1.892(8)	2.048(3)	2.089(4)
Ni–N(5)	1.889(7)	2.047(3)	2.058(4)
Ni–O(12)	1.855(7)	2.023(3)	2.012(3)
Ni–O(19)	1.864(7)	2.032(3)	2.047(3)
Ni–O(6)		2.169(3)	2.091(3)
Ni–O(8)		2.102(3)	2.145(11)
N(1)–C(2)	1.46(1)	1.458(6)	1.483(6)
C(2)–C(3)	1.49(1)	1.542(6)	1.504(8)
C(3)–C(4)	1.51(2)	1.533(6)	1.479(8)
C(4)–N(5)	1.45(1)	1.457(5)	1.483(6)
N(5)–C(20)	1.30(1)	1.304(5)	1.301(6)
C(20)–C(7)	1.42(1)	1.444(5)	1.439(6)
C(7)–C(11)	1.38(1)	1.422(6)	1.427(6)
C(11)–O(12)	1.27(1)	1.275(5)	1.265(5)
N(1)–C(70)	1.32(1)	1.305(5)	1.303(6)
C(70)–C(14)	1.44(1)	1.452(6)	1.451(7)
C(14)–C(18)	1.40(1)	1.424(5)	1.421(7)
C(18)–O(19)	1.30(1)	1.265(5)	1.256(5)
N(1)–Ni–N(5)	90.9(3)	91.9(1)	97.2(2)
N(1)–Ni–O(12)	168.9(3)	174.4(1)	172.6(2)
N(1)–Ni–O(19)	93.5(3)	90.5(1)	87.8(2)
N(5)–Ni–O(12)	94.8(3)	90.8(1)	89.8(2)
N(5)–Ni–O(19)	170.5(4)	175.4(1)	174.6(2)
O(12)–Ni–O(19)	82.2(2)	87.1(1)	85.2(1)
N(1)–Ni–O(6)		86.8(1)	91.2(2)
N(5)–Ni–O(6)		89.0(1)	86.8(1)
O(8)–Ni–O(6)		175.3(1)	174.0(4)
O(12)–Ni–O(6)		88.5(1)	91.5(1)
O(19)–Ni–O(6)		95.1(1)	91.4(1)
N(1)–Ni–O(8)		91.2(1)	90.2(3)
N(5)–Ni–O(8)		86.8(1)	87.3(4)
O(12)–Ni–O(8)		93.8(1)	87.9(3)
O(19)–Ni–O(8)		89.2(1)	94.4(4)
Some angles (°) between planes			
N(1)–Ni–O(19)			
O(12)–Ni–N(5)	12.7(3)	6.4(1)	3.0(2)
O(12)–Ni–O(19)			
N(1)–Ni–N(5)	13.7(3)	6.4(1)	3.0(2)
O(6)–Ni–N(1)			
O(8)–Ni–O(12)		5.0(1)	9.2(3)
N(1)–Ni–O(8)			
O(12)–Ni–O(6)		5.0(1)	9.1(3)
O(6)–Ni–N(5)			
O(8)–Ni–O(19)		3.1(1)	5.1(2)
N(5)–Ni–O(8)			
O(19)–Ni–O(6)		3.0(1)	5.1(2)

Estimated standard deviations (e.s.d.s) of the least significant digits are given in parentheses.

whereas **1b** has an approximate two-fold axis. The packing is quite different, and no significant interactions are observed. The anomalously high thermal motion observed for atoms C(15) and C(17) is ascribed mainly to the disorder of the dmso. In general the thermal parameters are larger than those for **1b** due to the data collection temperature: 120 K for **1b**, 298 K for **3b**.

Electrochemistry

Complexes and pro-ligands were studied by cyclic voltammetry in CH_2Cl_2 at different scan rates. The pro-ligands are irreversibly oxidized above 1.5 V. Complexes **4a** and **7a** are unstable in CH_2Cl_2 under the given conditions; they decompose and only ligand oxidation is observed. The aldimine complexes **11a–14a** and the ketoimine complexes **5a** and **9a** are irreversibly oxidized at 1.3 (**11a–14a**), 1.21 (**5a**) and 1.13 V (**9a**). The remaining complexes are quasi-reversibly oxidized, the half-wave potentials being listed in Table 3. The large ΔE values decrease with decreasing scan rate thus indicating the quasi-reversible nature of the process. They are, however, indicative of a two-electron transfer involving both the ligand and metal as demonstrated for similar systems by ESR spectroscopy of the oxidized products.[5c,8]

Nickel(II) in these complexes is stabilized compared with N_2O_2 Schiff-base complexes based on aromatic carbon cycles: ΔE = 100–133 mV, $E_{\frac{1}{2}}$ = 627–778 mV are reported for n = 2 or 3 complexes incorporating naphthalene,[5c] and ΔE = 110–212 mV, $E_{\frac{1}{2}}$ = 905–935 mV for substituted and unsubstituted *N,N'*-bis(salicylidene)-*o*-phenylenediamine complexes[8] {measured in dimethylformamide *vs.* Ag–AgCl [$E_{\frac{1}{2}}$(ferrocene) = 480 mV [5c]}.

Spectroscopic investigations in non-donor solvents ($CHCl_3$, $CDCl_3$)

For NMR and equilibrium data and electronic spectra see SUP 57154.

Proton NMR spectra. The chemical shifts observed are normal for diamagnetic compounds. When n = 3, however, the line broadening, indicates the presence of paramagnetic species. Spectra recorded in the range −50 to 50 °C show that the chemical shifts, especially of the methylene protons, H_a, closest to the nitrogen donor atom, are highly temperature dependent for the n = 3 complexes due to an increase in the paramagnetic isotropic Fermi contact shift with temperature, see Fig. 4. When n = 2 the chemical shift of H_a is practically temperature independent.

Thermodynamic parameters for the spin-equilibrium process. The chemical shifts of protons H_a were used to evaluate the equilibrium constants for the spin equilibrium process[3f] (see Experimental section) and ΔH and ΔS were derived from the van't Hoff plots (Table 4). The values of ΔH are within the range for nickel(II) complexes of tetradentate salicylaldimines linked by a biphenyl or naphthyl bridge[3a] (type 1) and are more positive than for the bis(bidentate Schiff-base) complexes based on salicylaldehydes and β-diketones[3b–e] (type 2). The ΔS value for **9a** is in the range for the type 2 complexes (10–25 J K^{-1} mol^{-1}). In general, however, the values of ΔS are significantly less positive than for both types 1 and 2 (10–55 J K^{-1} mol^{-1}) as probably no extra degree of rotational freedom for the ligand substituents is gained in the tetrahedral form. The *p*-chlorophenyl-substituted complex **6a** is more paramagnetic than the phenyl-substituted **5a** in accordance with the general trend that σ-electron-withdrawing substituents decrease the Lewis basicity of a ligand.[2d]

Electronic spectra. For the four-co-ordinate complexes D_{4h} symmetry is assumed. The ground state is $^1A_{1g}$ and the observed lowest-energy ligand-field band is assigned to the $^1A_{2g}$[9] and the higher-energy band to the $^1B_{1g}$ transition. A shoulder observed at ≈16 150 cm^{-1} for **2a** and **4a** is assigned to the ^1E_g transition, see Table 5.

Substitution effects are small compared with those of an increase in chain length. Thus red-shifts of about 1000 ($^1A_{2g}$) and 1600 cm^{-1} ($^1B_{1g}$) on going from n = 2 to 3 are ascribed to increased tetrahedral distortion from a planar geometry. Similar effects have been observed for the Schiff-base complexes incorporating aromatic carbon cycles.[1e,10a] Otherwise the ligand-field spectra for the latter[5c,10] differ considerably from those of the present complexes. A single ligand-field band between 17 000 and 18 500 cm^{-1} is considered to be a combination of all the expected transitions.[9a,10b] The spectrum of a complex of the salicylaldimine type, n = 2, was partly resolved by circular dichroism.[10c] Three bands of low intensity at around 18 000, 19 500 and 22 000 cm^{-1} were assigned to ligand-field transitions.[10c] Obviously the heteroaromatic pyrazole weakens the ligand-field strength compared with an aromatic carbon cycle.

For planar transition-metal complexes with more than six d electrons the energy of the d_{z^2} orbital is lower than predicted by

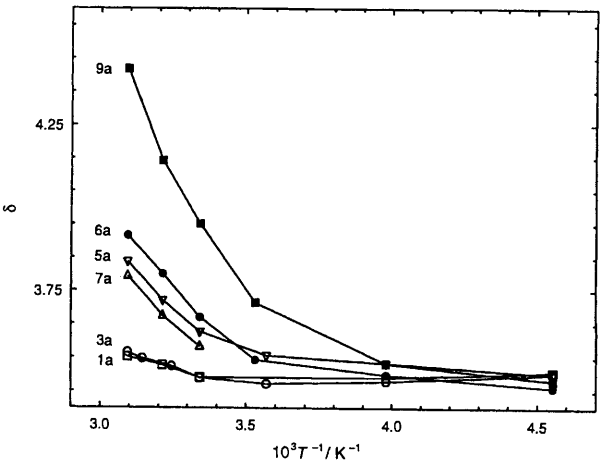

Fig. 4 Temperature-dependent ^1H NMR chemical shifts of protons H_a in complexes **1a**, **3a**, **5a**, **6a**, **7a** and **9a** in $CDCl_3$

Table 3 Voltammetric data[a] (V)

Complex	E_{ox}	E_{red}	ΔE	$E_{\frac{1}{2}}$
1a	1.28	1.10	0.18	1.19
2a[b]	1.26	1.16	0.10	1.21
3a	1.24	1.12	0.12	1.18
6a	1.25	1.08	0.17	1.17
8a	1.24	1.14	0.10	1.19
10a	1.21	1.09	0.12	1.15

[a] Measured at room temperature by cyclic voltammetry with platinum working and counter electrodes *vs.* Ag–AgCl as reference electrode. Sweep rate 0.100 V s^{-1}, 0.1 mol dm^{-3} NBu_4PF_6, 1 mmol dm^{-3} complex; $E_{\frac{1}{2}}$ (ferrocene) = 0.60 V. [b] Concentration: 0.5 mmol dm^{-3}. Complexes **4a** and **7a** are not stable, and **5a**, **9a** and **11a–14a** give irreversible couples under the given conditions.

Table 4 Thermodynamic parameters for the spin-equilibrium process[a]

	Complex					
Parameter	**1a**	**3a**	**5a**	**6a**	**7a**	**9a**
ΔH/kJ mol^{-1}	20.6	—	17.3	16.4	16.4	21.2
ΔS/J K^{-1}mol^{-1}	4.8	—	4.3	3.1	1.8	21.5
ΔG^b/kJ mol^{-1}	19.0	19.0	15.9	15.4	15.8	14.3

[a] Correlation coefficients of the van't Hoff plots: **1a**, −0.9988; **5a**, −0.9999; **6a**, −0.9997; **7a**, −0.9992; **9a**, −0.9995. [b] At 50 °C.

Table 5 Ligand-field transitions and parameters for the four-co-ordinate complexes in $CHCl_3$ at 20 °C[a]

Complex	Transition $^1A_{2g}$	Transition $^1B_{1g}$	e_σ	e_π	e_σ/e_π	Δ_1[b]
1a	15 825 (75)	20 365 (220)	7750	1205	6.4	18 430
2a[c]	15 675 (64)	20 245 (206)	7710	1215	6.3	18 270
3a	15 775 (76)	20 245 (240)	7710	1190	6.5	18 370
4a[c]	15 675 (76)	20 870 (sh) (309)	—	—	—	—
5a	15 530 (72)	20 000 (246)	7635	1195	6.4	18 125
6a	15 480 (72)	20 000 (245)	7635	1205	6.3	18 085
7a	15 530 (71)	20 000 (232)	7635	1195	6.4	18 125
8a	16 610 (93)	21 550 (415)	8105	1275	6.4	19 215
9a	15 725 (77)	20 080 (229)	7660	1165	6.6	18 320
10a	16 555 (87)	21 645 (388)	8135	1310	6.2	19 165
11a[d]	15 600 (≈75)	20 000 (≈255)	7635	1175	6.5	18 205
12a[d]	15 480 (≈70)	20 000 (≈225)	7635	1205	6.3	18 085
13a[d]	16 640 (≈95)	21 690 (≈380)	8150	1300	6.3	19 250
14a	16 665 (79)	21 550 (383)	8105	1265	6.4	19 255

[a] Energies in cm^{-1}, absorption coefficients listed in parentheses in dm^3 mol^{-1} cm^{-1}; sh = shoulder. [b] $\Delta_1 = E(d_{x^2} - d_{y^2}) - E(d_{xy}) = 3e_\sigma - 4e_\pi$. [c] $E(^1E_g) \approx 16\,150$ cm^{-1} for complexes **2a** and **4a**; $B = 650$ cm^{-1} was calculated for **2a** and estimated for the others. [d] The intensities are concentration dependent.

Table 6 Magnetic moments measured in $(CD_3)_2SO$ at 26 °C

Complex	μ/μ_B	Decrease* (%)
$[Cr(acac)_3]$	3.99(3)	2
1b	3.55(2)	0
2b	3.31(34)	1
3b	3.34(28)	1
4b	3.28(22)	2
5b	3.44(8)	1
6b	3.58(12)	2
9b	3.50(3)	7
11b	2.71—	7

Compounds not listed are not soluble enough for reliable Evans measurements; $\mu_B \approx 9.27 \times 10^{-24}$ J T^{-1}. * Decrease of moment measured at 90 °C.

simple ligand-field theory.[9,10a,b] A stabilizing effect from $3d_{z^2}$–4s mixing is assumed. When this assumption is included in the angular overlap model (AOM) together with the introduction of the parameter $e_{\sigma sd}$ which quantifies this effect.[9b] The parameters obtained are given in Table 5 (see Experimental section for the calculations). A value of $B = 650$ cm^{-1} was calculated for **2a** and estimated for the others; $C = 4B$ and $e_{\sigma sd} = 1.3e_\sigma$ have been assumed. The Lewis basicity of the ligands was evaluated from e_σ. It is similar to that of $n = 2$ Schiff bases based on salicylaldehydes and β-diketones.[9b] The π-donor properties, reflected in the magnitude of e_π, are stronger; $e_\sigma = 7000$–8000 and $e_\pi \approx 1000$ cm^{-1} were found for low-spin cobalt(II) complexes.[9b] The $n = 2$ ligands are the strongest Lewis bases and π donors. The larger Δ_1 values for the $n = 2$ complexes are in accord with the thermodynamics for the spin-equilibrium process. The simplifying assumptions made prevent detailed comparisons within the $n = 2$ and $n = 3$ series. However, the following observations can be made: (1) Δ_1 decreases with ΔH for the spin-equilibrium process as it should; (2) according to the magnitude of Δ_1, the ketoimine ligands in **1a** and **5a** are slightly stronger than the analogous aldimine ligands in **11a** and **12a**.

In D_{4h} symmetry the Laporte-forbidden ligand-field bands are expected to gain intensity with temperature.[11] The opposite temperature dependence observed for all ketoimine complexes is attributed to the actual lower symmetry[11] (C_2). As indicated by the ^1H NMR chemical shifts of the protons, the $n = 2$ ketoimine complexes are fully diamagnetic, and for these the temperature dependence cannot be due to a change in the low-spin population.

The bulky ketoimine complexes investigated in the present work do not self-associate. It was also observed in previous studies[1a,e,12] that sterically demanding ligands reduce or prevent the formation of paramagnetic oligomers. In contrast the aldimine complexes form self-association products in dry $CHCl_3$ as seen in the electronic spectra. The intensities of the singlet bands are concentration dependent, increasing with temperature as the concentration of oligomers is lowered. Dilute solutions (≈1 mmol dm^{-3}) have to be used to prevent precipitation of the green self-association products from the red solution. For **14a** the intensities of the singlet bands are practically temperature independent, and no concentration dependence is observed. The steric effect from the methyl substituent of the chain seems to diminish the self-association compared with the unsubstituted chain in **13a**.

Spectral data for the protonated pro-ligands and charge-transfer (c.t.) and intra-ligand transitions for selected complexes are presented in the Experimental section. The transition found at about 26 600 cm^{-1} for the $n = 2$ complexes is assigned to a $L_\pi \rightarrow M_\sigma^*$ c.t. transition. In this assignment the optical electronegativity of the ligand π orbital is 3.2 in accord with values for other π-donor ligands.[11] When $n = 3$ the pro-ligand spectrum changes little on complex formation with Ni^{II}.

Investigations in the donor solvent dmso

Adduct formation. Magnetic moments for the more soluble $n = 3$ complexes were measured in $(CD_3)_2SO$ by the Evans method[13] (Table 6). A significant drop in moment with temperature was observed for **9b** and **11b** compared with a paramagnetic standard $[Cr(acac)_3]$ (acac = acetylacetonate) measured under the same conditions. Apparently the two complexes lose axial ligand. The lower acidity of the aldimine complex may be attributed to competing molecular association.

Paramagnetically broadened resonances and isotropic shifts are observed in the ^1H NMR spectra (see SUP 57154). The isotropic shifts are small for the $n = 2$ complexes, and the chain protons are seen. This is an indication of the presence of diamagnetic species and of the weak acidity also seen in the electronic spectra (see below). When $n = 3$ the resonances of the protons of the chain, H_a and H_b, are not observed after addition of small amounts of $(CD_3)_2SO$ to a $CDCl_3$ solution of the complex, see Fig. 5 (o1 and o3 are the *o*-phenyl protons of R^1 and R^3, respectively).

One isosbestic point is seen in the electronic spectra as $CHCl_3$ solutions of complexes **1a**, **3a**, **5a**, **6a** and **9a** are titrated with dmso at room temperature (Fig. 6). The values of K_{2obs} and β_{obs} were evaluated from equation (3) and are given in Table 7. The intensity drop for $^1B_{1g}$ was used to determine the concentration of the low-spin form. As K_{2obs} appears highly concentration dependent in contrast with β_{obs}, it is concluded that the two species present are four- and six-co-ordinate complexes. A five-co-ordinate intermediate is not stable. Titration with dmso of the $n = 2$ ketoimine complexes in $CHCl_3$ results in decreased intensities of the singlet bands. Addition of small amounts of

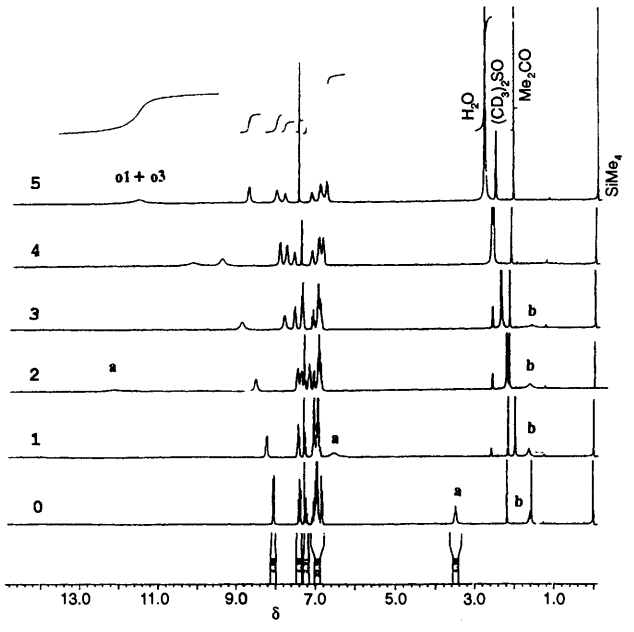

Fig. 5 Variation of the ^{1}H NMR spectrum of a 7.8 mmol dm^{-3} solution of complex **1a** in $CDCl_3$ upon addition of $(CD_3)_2SO$ at room temperature. Curves 0–5: 0, 20, 40, 60, 120 and 220 mg cm^{-3} $(CD_3)_2SO$

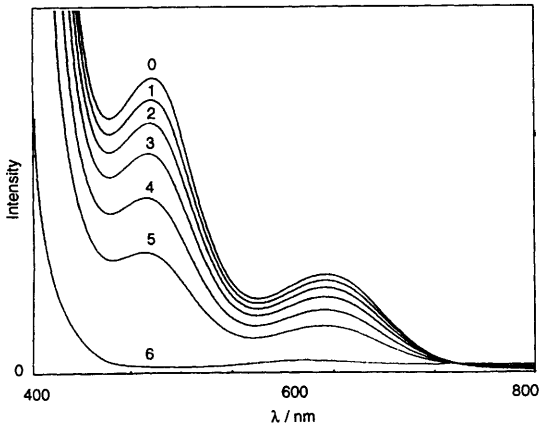

Fig. 6 Variation of the electronic absorption spectrum of complex **1a** in $CHCl_3$ upon addition of dmso at room temperature. Total nickel(II) concentration: 8.021 mmol dm^{-3}. Curves 0–5, 0, 0.703, 1.075, 1.395, 1.786 and 2.331 mol dm^{-3} dmso; 6, 8.021 mmol dm^{-3} solution of **1b** in dmso

Table 7 Evaluation of the co-ordination number x of complex **1a** titrated with dmso in $CHCl_3$ at room temperature by examination of the concentration dependence of K_{2obs} and β_{obs} *

$[B]_T$/mol dm^{-3}	[NiL]/mmol dm^{-3}	K_{2obs} (x = 1)/ dm^3 mol^{-1}	β_{obs} (x = 2)/ dm^6 mol^{-2}
0	8.021	—	—
0.703	6.845	0.245	0.350
1.075	6.268	0.261	0.244
1.395	5.495	0.330	0.238
1.786	4.386	0.465	0.262
2.331	3.023	0.711	0.307

* B = dmso; see equation (3) for the calculations.

dmso, however, results in precipitation. Equilibrium constants close to zero are found at room temperature.

Temperature-dependent gross equilibrium constants for the adduct formation were evaluated by the method described in the Experimental section, and ΔH_{dmso} and ΔS_{dmso} were derived from the van't Hoff plots (Table 8). The enthalpy change reflects the electronic part of the acidity: $-\Delta H_{dmso}$ decreases in the order (n = 3) 1,3-Ph_2 > 1-Ph-3-Me > 1-Me-3-Ph ≫ n =

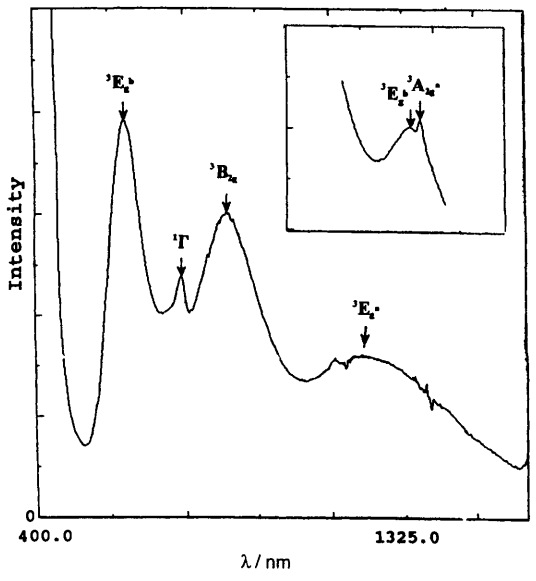

Fig. 7 Assignment of the electronic absorption spectrum of complex **6b** in dmso at 15 °C. The resolved $^3A_{2g}{}^a$ and $^3E_g{}^b$ bands for **7b** are seen in the inset

2, where the substituents are those on the pyrazolyl groups. The low acidity of the n = 2 complexes is attributed mainly to a strong ligand field in the four-co-ordinate parent complexes.[4] In general the order is in accord with the usual finding that a strong ligand field, evaluated here by ΔH for the spin-equilibrium process and by Δ_1, decreases the acidity;[2d,4,14] *e.g.* [Ni(salen)] (n = 2) does not add donor solvent whereas [Ni(salpd)] (n = 3) does.[4] The methyl substituents have no significant electron-releasing effect on the acidity of **3a**, while the electron-withdrawing chlorine substituent as expected[2b,d] increases the acidity of **6a** compared with that of **5a**. The diphenyl pyrazolyl n = 3 ketoimine complexes deviate from the expected order. They have, however, similar ligand-field strengths, and the reason may be that the systems with larger ligands, in spite of a slightly stronger ligand field, can better accommodate the extra charge from the axial ligands.

The steric part of the acidity is evaluated from the entropy change: ΔS_{dmso} is significantly more negative for the methyl-substituted **3a** than for the unsubstituted **1a**. A similar consequence for ΔS_{dmso} was expected, but not found, for the chlorine-substituted **6a** compared with **5a**.

Electronic spectra. The ligand-field transitions for the dmso adducts are given in Table 9(*a*), and a representative spectrum is shown in Fig. 7. Three to four well resolved triplet bands are observed corresponding to splitting of the octahedral $^3A_{2g} \longrightarrow {}^3T_{2g}$ and $^3A_{2g} \longrightarrow {}^3T_{1g}$ transitions; the assignment follows that for a tetragonal distortion.[15] The ground state is $^3B_{1g}$. The band $^3A_{2g}{}^a$, $^3E_g{}^b$ is in many spectra observed as a superposition of the two transitions. In some spectra the two bands are resolved, see Fig. 7, inset, for **7b**. When n = 2 the singlet bands are preserved with some lowering of intensity compared with those in the $CHCl_3$ spectra, and some preservation of the singlet bands is also observed in the spectra of **9b** and **12b**.

The AOM ligand-field parameters derived from the electronic spectra are in Table 9(*b*) (see Experimental section). In the calculations $^3E_g{}^b$ is in general estimated to be blue shifted by 20 nm (525 cm^{-1}) relative to $^3A_{2g}{}^a$. The calculations yield d_π; values for e_σ and e_π are derived from the assumption[9a] that the relation $e_{\sigma L}/e_{\pi L}$ is as for the four-co-ordinate parent complex. Observed [Table 9(*a*)] and calculated transition energies (see Experimental section) fall within the range found for other tetragonally distorted nickel(II) complexes.[11]

The large tetragonal distortion observed in the spectra is

Table 8 Thermodynamic parameters for dmso co-ordination[a]

Parameter	**1a** ⇌ **1b**	**3a** ⇌ **3b**	**5a** ⇌ **5b**	**6a** ⇌ **6b**	**9a** ⇌ **9b**
ΔH_{dmso}/kJ mol^{-1}	−23.9(7)	−27(2)	−15.1(5)	−16.9(4)	−10(1)
ΔS_{dmso}/J K^{-1} mol^{-1}	−91(2)	−107(8)	−65(2)	−60(1)	−57(4)
ΔG (25 °C)/kJ mol^{-1}	3.2(7)	5(2)	4.1(5)	0.91(4)	7(1)
Correlation coefficient[b]	0.9980	0.9914	0.9973	0.9982	0.9646

[a] e.s.d.s of the least significant digits are given in parentheses. [b] Of the van't Hoff plot.

Table 9 Ligand-field data for the dmso-solvated six-co-ordinate complexes at 15 °C

(*a*) Transitions[a]

Complex	^3E_g[a]	$^3B_{2g}$	$^1\Gamma$	$^3A_{2g}$[a], ^3E_g[b]	$^1A_{2g}$	$^1B_{1g}$
1b	8 330	11 440	13 210	16 285	—	—
	(3.4)	(5.9)	(5.1)	(9.2)		
2b	8 330	11 350	13 193	16 205[b]	—	—
	(4.9)	(8.8)	(3.0)	(7.9)		
3b	8 330	11 495	13 193	16 260	—	—
	(5.0)	(10.4)	(11.4)	(13.3)		
4b	8 330	11 350	13 193	16 205[b]	—	—
	(3.2)	(6.0)	(3.3)	(8.3)		
5b	8 200	11 440	13 158	16 130[b]	—	—
	(4.0)	(7.1)	(6.0)	(10.2)		
6b	8 200	11 390	13 158	16 105	—	—
	(4.2)	(8.2)	(6.3)	(11.0)		
7b	—	≈11 500	13 176	15 950[b]	—	—
			(6.3)	(10.8)		
9b	8 200	11 175	13 263	15 925	—	20 200 (sh)
	(6.0)	(10.1)	(6.6)	(22.3)		(39.5)
12b	8 000	11 025	13 175	15 875	—	20 000 (sh)
	(4.5)	(7.7)	(7.8)	(13.7)		(25.3)
13b	8 000	12 345	13 298	16 665[c]	16 980	21 835
	(6.1)	(14.1)	(14.4)		(77.3)	(296)
14b	8 000	12 345	13 298	16 665[c]	16 980	21 740
	(1.7)	(4.9)	(4.8)		(76.3)	(354)

(*b*) Parameters[d]

n	*B*	d_π[e]	$e_{\sigma L}$	$e_{\sigma B}$	$e_{\pi L}$	$e_{\pi B}$[e]
3	705(5)	645(25)	4 775(70)	2 815(50)	750(20)	1 390(35)
2	720(0)	950(0)	5 210(20)	2 905(20)	820(15)	1 770(15)

[a] Energies are in cm^{-1}, absorption coefficients (in parentheses) in dm^3 mol^{-1} cm^{-1}. Complexes **7b**, **8b** and **10b** are sparingly soluble; **11b** was not measured due to lack of material. [b] Two maxima at a distance of ≈20 nm are observed; the average value is listed. [c] Estimated value. [d] The average values (in cm^{-1}) for $n = 3$ and $n = 2$ complexes have been listed (e.s.d.s in parentheses). [e] Uncertain.[15]

obvious from the small value of quotient $e_{\sigma B}/e_{\sigma L}$. The average values are 59 ($n = 3$) and 55% ($n = 2$). This quotient reflects the weak Lewis basicity of dmso compared with that of the Schiff-base ligand. In the model used the uncertainties of $e_{\pi B}$ are expected to be rather large.[15] Dimethyl sulfoxide seems, however, to be a fairly strong π donor.

The c.t. and intra-ligand transitions for representative complexes are given in the Experimental section. Adduct formation seems to reduce the ligand conjugation. The low-energy π ⟶ π* transition at about 28 570 cm^{-1} observed for the protonated pro-ligand and for the four-co-ordinate complex moves to higher energy. When $n = 2$ the UV region is dominated by the four-co-ordinate complex.

Investigations in the donor solvent pyridine

Adduct formation. Six-co-ordinate complexes are formed in pyridine solutions according to the elemental analysis of **1c**. A five-co-ordinate intermediate seems, however, to be fairly stable. Isosbestic points are not seen in the electronic spectra as $CHCl_3$ solutions of **1a** are titrated with diluted pyridine (Fig. 8). Values of K_2, K_3 and β, see equation (3), were obtained from the titration data (Table 10). The intensity drop of band $^1B_{1g}$ was used for concentration determinations; K_2 was calculated at the lowest, β at the highest pyridine concentration on the assumption that the four- and five-co-ordinate species dominate at low pyridine concentrations [Fig. 8(*a*)] and the four- and six-co-ordinate species at high pyridine concentrations [Fig. 8(*b*)]. The magnitude and order ($K_3 \gg K_2$) of the equilibrium constants (see SUP 57154) are in good agreement with results from previous measurements of pyridine co-ordination to $Ni^{II}N_2O_2$ complexes in two distinguishable steps.[1f,2b,d]

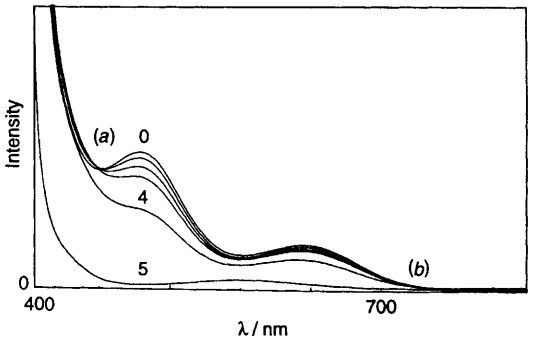

Fig. 8 Variation of the electronic absorption spectrum of complex **1a** in $CHCl_3$ upon addition of pyridine at room temperature. Total nickel(II) concentration: 2.436 mmol dm^{-3}. Curves: 0–4, 0, 3.440, 6.880, 10.316 and 20.616 mmol dm^{-3} pyridine; 5, 2.436 mmol dm^{-3} solution of **1c** in pyridine

Electronic spectra. The ligand-field spectral data [see Table 11(*a*)] show that tetragonal distortions from octahedral

Table 10 Evaluation of the co-ordination number x of complex **1a** titrated with pyridine in $CHCl_3$ at room temperature and the thermodynamic parameters by examination of the concentration dependence for K_{2obs} and β_{obs} [a]

$[B]_T$/mmol dm^{-3}	[NiL]/mmol dm^{-3}	K_{2obs} (x = 1)/ dm^3 mol^{-1}	10^{-3} β_{obs} (x = 2)/ dm^6 mol^{-2}
0	2.436	—	—
3.440	2.332	13.4	4.27
6.880	2.177	17.9	2.94
10.316	2.027	20.4	2.24
10.308	2.005	21.8	2.41
20.616	1.427	36.1	2.04

[a] B = Pyridine. See equation (3) for the calculations. $K_2 \approx 10$ dm^3 mol^{-1}, $\beta \approx 2 \times 10^3$ dm^6 mol^{-2}, $K_3 = \beta/K_2 \sim 2 \times 10^2$ dm^3 mol^{-1}, ΔG (25 °C) ≈ -19 kJ mol^{-1}.

symmetry are small, especially when $n = 3$. Three bands are assigned to $^3B_{2g}$, $^3A_{2g}{}^a$, $^3E_g{}^b$ and $^3E_g{}^c$ (the latter for **12c** only), and the usual [11,15] spin-forbidden bands are observed.

The AOM ligand-field parameters derived from the spectra are given in Table 11(*b*). A value $B = 700$ cm^{-1} was calculated for **12c**, with $^3A_{2g}{}^a = {}^3E_g{}^b$, and estimated for the others. For the $n = 2$ complexes an iterative procedure was used (see Experimental section). Observed [Table 11(*a*)] and calculated transition energies (see Experimental section) fall within the range of those for tetragonally distorted nickel(II) complexes.[11]

The larger $e_{\sigma B}/e_{\sigma L}$ ($n = 3$, 79%; $n = 2$, 73%) values than found for the dmso adducts show that pyridine is a stronger Lewis base than dmso in accordance with the thermodynamic measurements. The π-donor properties found for pyridine are probably significant. Such properties are expected; $e_{\pi L}$ values of ≈ 100 cm^{-1} and $e_{\pi B}$ values of more than 1000 cm^{-1} have been reported.[11,16]

Comparisons of thermodynamics and ligand-field parameters show that dmso is a much weaker ligand compared with pyridine than could be predicted from previous experiments.[2d,17] Similar donor numbers are reported for dmso (29.8) and pyridine (33.1) for four-co-ordinate 3d transition-metal complexes with one *N*,*N*′-substituted ethane-1,2-diamine and one acetylacetonate ligand.[17] The acidity of diamagnetic Ni^{II} with a similar saturated–unsaturated mixed ligand system has been investigated, and equilibrium constants of comparable size were found for dmso and pyridine.[2d] Our experiments confirm that the observed Lewis basicity of an axial ligand strongly depends on the metal π interaction with the in-plane ligands.[17]

Experimental

Materials

Chemicals for the preparations were reagent grade and commercially available, and were used without further purification. Pyridine and dmso for solvation experiments were spectroscopic grade and dried over 4 Å sieves; $CHCl_3$ and CH_2Cl_2 used as non-donor solvents were boiled over phosphorus pentaoxide and distilled immediately before use.

Preparations

The pyrazolones[18a] and benzoylpyrazolones[18b] used as starting materials and the Schiff-base ketoimines[18c] were prepared according to literature methods.

Aldimines. *Method 1.* 5-Hydroxy-3-methyl-1-phenylpyrazole-4-carbaldehyde used as starting material[18d] was kindly provided by the Department of Organic Chemistry, Leipzig University. The Schiff bases corresponding to complexes **12** and **13** were prepared by the method used for the ketoimines.

Method 2. The appropriate *o*-chloropyrazolecarbaldehydes (5 mmol) corresponding to complexes **11**, **12** and **14** prepared according to literature methods[18a] and 33% aqueous NaOH (4 cm^3) were stirred in 99.9% EtOH (25 cm^3) for 10–12 h at reflux temperature. Sodium chloride was filtered off. Propane-1,3-diamine (2.5 mmol) was added to the filtrate, and the solution stirred for 10–12 h. After cooling, the excess of base was neutralized by formic acid. The solution was concentrated, the sodium formate was filtered off, and the filtrate evaporated to dryness. The residue was dissolved in $CHCl_3$, and the product precipitated with 96% EtOH. The practically colourless pro-ligands were purified by preparative TLC, using MeOH–CH_2Cl_2 (1:9) as eluent. One band yielded the unexpected $CHMeCH_2$ derivative: ^1H NMR ($CDCl_3$). δ (chain) 0.982 (CH_3), 2.618 (CH) and 2.175, 3.079 (CH_2). Chemical shifts $\delta(H_a)$ for selected protonated pro-ligands (numbered as in complexes) 3.358 (**1**), 3.426 (**3**), 3.235 (**5**), 3.257 (**6**), 3.239 (**7**) and 3.318 (**9**). UV ($CHCl_3$): λ/nm (ε/dm^3 mol^{-1} cm^{-1}) (in general) ≈275 (25 000–35 000), ≈315 (24 000–41 000) and ≈350 (sh) (≈11 000); (specific): 270 (50 000), 318 (29 000) and 391 (8290) (**4**); 276 (55 500) and 352 (11 500) (**9**); 302 (19 500) and 353 (11 000) (**10**).

Table 11 Ligand-field data for the pyridine solvated six-co-ordinate complexes at 10 °C

(*a*) Transitions [a]

Complex	$^3B_{2g}$	$^1\Gamma^a$	$^3A_{2g}{}^a$,$E_g{}^b$	$^1\Gamma^b$
1c	10 660	12 660	17 300	—
	(11.5)	(4.2)	(13.1)	
3c	10 625	12 660	17 155	—
	(12.2)	(4.4)	(13.3)	
4c	10 580	12 660	17 100 (sh)	—
	(13.2)	(4.1)	(16.0)	
5c	10 660	12 660	17 155	21 280 (sh)
	(11.9)	(4.1)	(15.1)	(11.2)
6c	10 605	12 660	17 155	—
	(11.9)	(3.8)	(14.6)	
7c	10 660	12 660	17 180	—
	(8.6)	(3.3)	(11.5)	
8c	12 180	12 955	18 380	20 660
	(34.4)	(29.6)	(20.0)	(12.1)
9c	10 515	12 660	17 065	—
	(11.1)	(3.8)	(13.2)	
10c	11 890	12 920	18 050	20 535
	(32.8)	(24.1)	(19.7)	(8.3)
12c	10 695	12 740	17 360	22 120 (sh) [b]
	(12.6)	(4.7)	(15.2)	(42.2)
13c	11 975	12 905	17 955	21 370
	(32.4)	(26.7)	(17.6)	(13.7)
14c	11 960	12 885	18 050	21 275
	(37.9)	(29.5)	(17.8)	(8.1)

(*b*) Parameters [c]

n	B	$d_\pi{}^d$	$e_{\sigma L}$	$e_{\sigma B}$	$e_{\sigma L}$	$e_{\pi B}{}^d$
3	700	−130(30)	4 475(40)	3 555(55)	700(15)	570(30)
2	720	185(45)	5 070(40)	3 710(80)	800(15)	990(50)

[a] Energies in cm^{-1}, absorption coefficients (in parentheses) in dm^3 mol^{-1} cm^{-1}. Complexes **2c** and **11c** were not measured due to lack of material. [b] $^3E_g{}^c$. [c] The average values (in cm^{-1}) for $n = 3$ and $n = 2$ complexes have been listed (e.s.d.s in parentheses). [d] Uncertain.[15]

Complexes. The following general procedure was used. A suspension of the protonated pro-ligand (0.15 mmol) was stirred in 2-methoxyethanol (3–5 cm^3) and heated to reflux temperature. Anhydrous nickel(II) acetate (0.15 mmol) was added. The reaction mixture was kept at reflux temperature for 5 min, and the olive-green or red product was filtered off while the suspension was still hot. Some complexes were recrystallized from dry $CHCl_3$. Charge-transfer and intra-ligand transitions for selected complexes: λ/nm (ε/dm^3 mol^{-1} cm^{-1}) ($CHCl_3$) 259 (73 000), 273 (sh) (64 200), 325 (sh) (16 900) and 350 (sh) (10 500) (**1a**); 259 (37 200), 312 (20 100) and 347 (9700) (**5a**); 278

(sh) (36 600), 310 (sh) (19 160) and 350 (11 400) (**9a**); 270 (sh) (55 000), 311 (15 600), 346 (10 000) and 375 (8200) (**10a**); 271 (77 000), 315 (20 400) and 350 (sh) (11 200) (**11a**); 270 (sh) (59 000), 315 (12 700), 347 (8000) and 378 (7350) (**14a**); (dmso) 266 (65 000) and 320 (sh) (14 300) (**1b**); 269 (54 100) and 316 (sh) (14 800) (**5b**); 258 (28 800), 273 (27 600) and 329 (14 300) (**9b**); 274 (55 900) and 310 (sh) (18 100) (**11b**); 259 (45 500), 305 (sh) (11 200), 340 (sh) (6030) and 371 (5090) (**14b**).

Physical measurements

To check the reversibility of the investigated processes all temperature-dependent experiments except the low-temperature ^{1}H NMR measurements were carried out in both directions.

Proton and ^{13}C NMR spectra were obtained on Bruker AC250P, Varian unity-200, or Varian unity-400 spectrometers. Methanol was used for temperature calibration at low temperature, ethylene glycol at high temperature. The uncertainty of the temperature is 1 °C. The assignments were accomplished by comparisons between the systems, by titration of $CDCl_3$ solutions of complex **1a** with $(CD_3)_2SO$, and by selective decoupling of single protons. Magnetic susceptibilities of the $(CD_3)_2SO$-solvated complexes were measured by the Evans method[13] using acetone and $SiMe_4$ as internal and external standards. The two standards yielded consistent results. Electronic absorption spectra were obtained in a 1 cm quartz cuvette on a thermostatted Shimadzu UV-3100 apparatus. The maximum uncertainty of the temperature is 1.5 °C (at 90 °C). Electrochemical data were collected in CH_2Cl_2, under nitrogen by cyclic voltammetry. Ferrocene was used as external standard. The electrolyte, NBu_4PF_6, pro-ligands and complexes were dried in vacuum before use. The solvent with electrolyte was scanned before measurements to check the purity of the solvent, see Table 3 for details. The electron-impact mass spectra were obtained on a Finigan Mat SSQ710 or a Varian Mat 311A apparatus. Elemental analyses were performed at the H.C. Ørsted Institute, University of Copenhagen. All complexes except **12d** were dried in vacuum (24 h) before elemental analyses.

Determination of K_1 (T)

Equilibrium constants for the spin equilibrium (1) of the soluble ketoimine complexes were evaluated from the temperature-dependent $CDCl_3$ ^{1}H NMR spectra using equation (4)[3f] for the paramagnetic isotropic Fermi-contact shift of H_a. This is in

$$\delta_{a,obs} = -A_a N_{hs} \gamma_e h S(S+1)\, 10^6/(3\gamma_H kT) + \delta_{a,dia} \qquad (4)$$

the form presented in ref. 19(*a*). The coupling constant A_a is in units of Hz (1 G = 2.8 MHz), $\delta_{a,obs}$ is the observed shift (in ppm), $\delta_{a,dia}$ the shift of the diamagnetic reference (in ppm).[3f] The other symbols have their usual meanings. The diamagnetic reference is the chemical shift of the free pro-ligand in $CDCl_3$. The substitution of a known coupling constant for A_a yields N_{hs} and K_1; A_a = 3.5 MHz found[19b] for n = 4 complexes of Ni^{II} was used.

Determination of β(T)

Temperature-dependent gross equilibrium constants for the adduct formation were derived from the electronic spectra for selected complexes [equation (3)]. The temperature-dependent intensities of the $^1B_{1g}$ band were used for concentration determinations. All measurements were performed three or four times with total concentrations of Ni^{II} = 3–7 mg cm^{-3} (c_{Ni}) and dmso = 50–60 mg cm^{-3} (c_B). The constant β was determined at 22 °C for solutions of known c_{Ni} and c_B. The temperature dependence for β was then found for solutions of known c_B after the determination of c_{Ni} at 22 °C: [B] ≈ c_B was assumed, and equation (3) was used in (5).

$$\beta = [NiLB_2]/[NiL][B]^2 = (c_{Ni} - [NiL])/[NiL][B]^2 \quad (5)$$

Ligand-field parameters

Ligand-field analyses were made in the AOM approximation[9,15] assuming D_{4h} symmetry. As the electronic spectra were recorded in solution they were treated by a simple isotropic model.

For the four-co-ordinate complexes the ground state is $^1A_{1g}$ and three absorption bands are expected with the energies[9c,d] $E(^1B_{1g}) = 2e_\sigma + e_{\sigma sd} - C - 4B$; $E(^1E_g) = 3e_\sigma - 2e_\pi - C - 3B$ and $E(^1A_{2g}) = 3e_\sigma - 4e_\pi - C$, where C and B are the Racah interelectronic repulsion parameters ($C/B \approx 4$),[9a] e_σ and e_π are the AOM parameters, and $e_{\sigma sd}$ is a parameter describing the stabilization of the d_{z^2} orbital due to 4s–3d mixing. The size of this parameter is about e_σ.[9c] For the six-co-ordinate complexes the ground state is $^3B_{1g}$, and six transitions are expected with energies[15] $E(^3E_g{}^a) = \Delta_1 + \Delta_2 - \Delta_3 + 3B$, $E(^3B_{2g}) = \Delta_2$, $E(^3A_{2g}{}^a) = \Delta_2 - \Delta_3 + 12B$, $E(^3E_g{}^b) = \Delta_1 + \Delta_2 + 9B$, $E(^3E_g{}^a) = \Delta_1 + 2\Delta_2 - \Delta_3 + 3B$ and $E(^3A_{2g}{}^b) = 2\Delta_1 + 2\Delta_2 - \Delta_3 + 3B$. Relations to the AOM parameters and to the McClure parameter d_π are $\Delta_1 = -2(e_{\pi B} - e_{\pi L}) = -2d_\pi$, $\Delta_2 = 3e_{\sigma L} - 4e_{\pi L}$ and $\Delta_3 = -2(e_{\sigma B} - e_{\sigma L})$. Configuration interactions were not corrected for.

For the pyridine-solvated n = 2 complexes an iterative procedure was used to derive the ligand-field parameters. (1) A value B = 700 cm^{-1} results in calculated $^3E_g{}^a$ energies red-shifted by less than 500 cm^{-1} relative to $^3B_{2g}$. The appearance of the spectra suggests larger red-shifts. (2) For **14c** an estimated red-shift of 1000 cm^{-1} for $^3E_g{}^a$ and the observed $^3B_{2g}$ and $^3A_{2g}{}^a = {}^3E_g{}^b$ yield B = 730 cm^{-1}. (3) With the estimated $^3E_g{}^a$, the observed $^3B_{2g}$ and $^3E_g{}^b$, and B = 720 cm^{-1}, the position of $^3A_{2g}{}^a$ is calculated to be red-shifted 180 cm^{-1} relative to $^3E_g{}^b$. (4) This red-shift and B = 720 cm^{-1} were introduced for the remaining n = 2 complexes.

Calculated transition energies: dmso-solvated complexes, $^3E_g{}^c$ ≈19 800, n = 3; ≈20 400, n = 2; $^3A_{2g}{}^b$ ≈18 500 cm^{-1}; pyridine-solvated complexes, $^3E_g{}^a$ ≈11 100, n = 3; ≈11 550, n = 2; $^3E_g{}^c$ ≈22 000, n = 3; ≈24 000, n = 2; $^3A_{2g}{}^b$ ≈22 500, n = 3; ≈23 000 cm^{-1}, n = 2.

Crystallography

Details of the crystallographic determinations are listed in Table 12. The refinements were performed on F in every case. The remaining electron density, $\Delta\rho_{max}$, is located at distances < 1.35 Å from the metal atom. The plotting program ORTEP II[20a] was used for the diagrams.

Complexes 1a and 1b. An Enraf-Nonius CAD-4F diffractometer was used for intensity measurements. Data were corrected for Lorentz-polarization effects, and for absorption.[20b] The program XTAL 3.2[20c] (unless otherwise mentioned) was used to solve the structures and for the refinements. Remaining atoms were found in subsequent Fourier-difference electron-density (Δρ) maps. Block-diagonal least-squares refinement employing anisotropic thermal parameters for all non-hydrogen atoms and isotropic thermal parameters for most hydrogen atoms was used to convergence.

For complex **1a** red crystals were grown from chloroform. Preliminary oscillation and Weissenberg photography suggested the triclinic system, and cell constants were obtained by least-squares refinement from the setting angles of 25 reflections centred at positive and negative θ in the range 11–14°. Intensities were measured at room temperature. The intensity of a standard reflection was measured every 3 h and a

Table 12 Crystal data and details of data collection and structure refinement for complexes **1a**, **1b** and **3b**

	1a	**1b**	**3b**
Formula	$C_{47}H_{36}N_6NiO_2 \cdot 0.5CHCl_3$	$C_{47}H_{36}N_6NiO_2 \cdot 2C_2H_6OS$	$C_{49}H_{40}N_6NiO_2 \cdot 2C_2H_6OS$
M	835.230	931.808	891.77
Crystal system	Triclinic	Monoclinic	Triclinic
Space group	$P\bar{1}$	$P2_1/n$	$P\bar{1}$
a/Å	11.9354(9)	12.530(1)	12.811(3)
b/Å	13.153(3)	10.000(2)	11.145(3)
c/Å	13.768(1)	36.779(4)	19.958(5)
α/°	77.090(2)	—	101.04(2)
β/°	74.019(1)	96.766(8)	78.18(2)
γ/°	86.250(2)	—	67.84(2)
U/Å^3	2025(2)	4576(1)	2467(1)
Crystal size/mm	0.164 × 0.294 × 0.425	0.080 × 0.160 × 0.600	0.28 × 0.28 × 0.026
Developed forms	{100} {010} {001}	{100} {010} {001}	{100} {010} {001}
D^a/g cm^{-3} (298 K)	1.370	1.299	1.200
Z	2(+1 $CHCl_3$)	4	2
Radiation (λ/Å)	Mo-Kα (0.710 73)	Cu-Kα (1.541 78)	Mo-Kα (0.710 73)
μ/cm^{-1}	6.255	5.404	5.164
Transmission factors	0.8190–0.9113	0.9025–0.9619	0.9026–0.9997
θ Limits/°	2–26	1–75	0–23
Octants collected	h ≥ 0	h and $k \geq 0$	$k \geq 0$
Standard reflections	−6 4 −1	1 0 3, 0 2 0	4 −2 3, 3 3 −1
Fall-off in intensity (%)	2.2	5.6	8.5
No. unique data	7523	8962	6449
No. data with $I/\sigma(I) > 2.5$	6130	8506	4866
No. variables	552	762	613
R^b	0.088	0.074	0.060
R'^c	0.124	0.090	0.076
$\Delta\rho_{max}$, $\Delta\rho_{min}$/e Å^{-3}	1.83(1), 1.88(1)	1.5, −1.5	0.5, −0.7

[a] Measured by the flotation method (calculated for complex **3b**). [b] $R = \Sigma(|F_o| - |F_c|)/\Sigma|F_o|$. [c] $R' = [\Sigma w(|F_o| - |F_c|)^2/\Sigma w |F_o|^2]^{\frac{1}{2}}$. Weights $w^{-1} = \sigma(F^2)$ or $\{[\sigma_c(F^2) + 1.04F^2]^{\frac{1}{2}} - |F|\}^2$ for complex **3b**.

decay of 2.2% corrected for. Direct methods (SHELXS 86[20d]) in the space group $P1$ followed by an integrated Patterson and direct methods procedure (XTAL 3.2) in $P\bar{1}$ were used to solve the structure. The chloroform molecule is disordered; its atoms, given an occupation parameter of 50%, were fixed in the final cycles of the refinement, and a few hydrogen atoms, not seen in the Δρ maps, were placed in geometrically idealized positions (C–H 0.96 Å) and given a single isotropic thermal parameter (0.10 Å^2).

Light green crystals of complex **1b** were grown from chloroform–dmso (1:1). The monoclinic system was suggested and cell constants were obtained by least-squares refinement from the setting angles of 18 reflections centred at positive and negative θ in the range 38–46°. Intensities were measured at 122 K. The intensities of two standard reflections were measured every 10 000 s and a decay of 5.6% corrected for. The space group $P2_1/n$ was deduced from systematic absences. Direct methods were used to solve the structure. One dmso ligand is disordered. The occupation parameters for the sulfur atom and connected methyl groups were refined to 0.66 for the major component and 0.34 for the minor. The methyl protons of the dmso ligand, not seen in the Δρ maps, were placed in geometrically idealized positions (C–H 0.96 Å) and given a single isotropic thermal parameter (0.07 Å^2).

Light green crystals of complex **3b** were grown from chloroform–dmso (1:1). Preliminary cell dimensions and the space group were obtained from precession and Weissenberg films. The unit cell was refined using the setting angles from 24 reflections centred at positive and negative θ in the range 20–26°. A HUBER diffractometer was used for this and for the intensity measurements. Two standard reflections were measured every 50 and a decay of about 9% corrected for. Step scans of 50 points were collected, integrated[20e] and the intensities corrected for Lorentz-polarization effects. Absorption corrections were done by Gaussian integration. The program SHELX 86 was used for solving the structure. Full-matrix least-squares methods were used for the refinement of coordinates and anisotropic thermal parameters for all non-hydrogen atoms. Hydrogen atoms were introduced at calculated positions confirmed by Fourier-difference maps. One dmso entity is disordered. Constraints[20f] forcing both dmso groups to have identical geometries were introduced. The occupation parameters were refined to 0.59 for the major component and 0.41 for the minor.

Atomic coordinates, thermal parameters, and bond lengths and angles have been deposited at the Cambridge Crystallographic Data Centre (CCDC). See Instructions for Authors, *J. Chem Soc., Dalton Trans.*, 1996, Issue 1. Any request to the CCDC for this material should quote the full literature citation and the reference number 186/140.

Acknowledgements

We gratefully acknowledge Professor A. Ceulemans, University of Leuven, for helpful discussions (A. la C.), Mr. C. Buch, Mrs. B. Haack, Mrs. I. Johansen, Mr. T. Jensen, Mrs. I. Pedersen and Mr. O. T. Sørensen, Odense University, and Mrs. B. Heinrich, Mrs. T. Meinel and Mrs. J. Ortwein, Leipzig University, for technical assistance. Mr. F. Hansen and Dr. S. Larsen, University of Copenhagen, are acknowledged for the data collection and reduction for complex **1b**, Mr. M. Bak, Mr. N. P. Andersen and Mr. M. Sielemann, Aarhus University, for their participation in the crystal structure determination of **3b**, Professor H. Toftlund, Odense University, for providing laboratory facilities (A. la C.), and the Danish Natural Science Research Council and the Carlsberg Foundation for the diffractometers (R. H. and O. S.).

References

1 (*a*) R. H. Holm and K. Swaminathan, *Inorg. Chem.*, 1962, **1**, 599; (*b*) R. H. Holm and K. Swaminathan, *Inorg. Chem.*, 1963, **2**, 181; (*c*) R. H. Holm, G. W. Everett, jun., and A. Chakravorty, *Prog. Inorg. Chem.*, 1966, **7**, 83; (*d*) W. C. Hoyt and G. W. Everett, jun., *Inorg.*

Chem., 1969, **8**, 2030; (*e*) G. M. Mockler, G. W. Chaffey, E. Sinn and H. Wong, *Inorg. Chem.*, 1972, **11**, 1308; (*f*) M. Schumann, A. von Holtum, K. J. Wannowius, and H. Elias, *Inorg. Chem.*, 1982, **21**, 606.
2 (*a*) L. Sacconi, P. Nanelli, N. Nardi and U. Campigli, *Inorg. Chem.*, 1965, **4**, 943; (*b*) D. R. Dakternieks, D. P. Graddon, L. F. Lindoy and G. M. Mockler, *Inorg. Chim. Acta*, 1973, **7**, 467; (*c*) M. Schumann and H. Elias, *Inorg. Chem.*, 1985, **24**, 3187; (*d*) A. Taha, V. Gutmann and W. Linert, *Monatsh. Chem.*, 1991, **122**, 327.
3 (*a*) M. J. O'Connor, R. E. Ernst and R. H. Holm, *J. Am. Chem. Soc.*, 1968, **90**, 4561; (*b*) M. J. O'Connor, R. E. Ernst and R. H. Holm, *J. Am. Chem. Soc.*, 1968, **90**, 5735; (*c*) R. E. Ernst, M. J. O'Connor and R. H. Holm, *J. Am. Chem. Soc.*, 1967, **89**, 6104; (*d*) D. H. Gerlach and R. H. Holm, *J. Am. Chem. Soc.*, 1969, **91**, 3457; (*e*) G. W. Everett, jun. and R. H. Holm, *Inorg. Chem.*, 1968, **7**, 776; (*f*) R. H. Holm, *Acc. Chem. Res.*, 1969, **2**, 307.
4 S. Yamada, *Coord. Chem. Rev.*, 1966, **1**, 415.
5 (*a*) F. Akhtar and M. G. B. Drew, *Acta Crystallogr., Sect. B*, 1982, **38**, 1149; (*b*) M. G. B. Drew, R. N. Prasad and R. P. Sharma, *Acta Crystallogr., Sect. C*, 1985, **41**, 1755; (*c*) M. A. A. F. de C. T. Carrondo, B. de Castro, A. M. Coelho, D. Domingues, C. Freire and J. Morais, *Inorg. Chim. Acta*, 1993, **205**, 157; (*d*) F. Akhtar, *Acta Crystallogr., Sect. B*, 1981, **37**, 84; (*e*) A. G. Manfredotti and C. Guastini, *Acta Crystallogr., Sect. C*, 1983, **39**, 863.
6 W. Guo-Xiong, L. Qin, Z. Cheng and J. Huaxue, *J. Struct. Chem.*, 1989, **8**, 278 (in Chinese); H.-J. Krüger and R. H. Holm, *J. Am. Chem. Soc.*, 1990, **112**, 2955; J. M. Stewart, E. C. Lingafelter and J. D. Breazeate, *Acta Crystallogr.*, 1961, **14**, 888; Y. Elerman and M. Kabak, *Acta Crystallogr., Sect. C*, 1993, **49**, 1905.
7 F. H. Allen, O. Kennard, D. G. Watson, L. Bremmer, A. G. Orpen and R. Taylor, *J. Chem. Soc., Perkin Trans. 2*, 1987, S1.
8 B. de Castro and C. Freire, *Inorg. Chem.*, 1990, **29**, 5113.
9 (*a*) L. G. Vanquickenborne, A. Ceulemans, D. Beyens and J. J. McGarvey, *J. Phys. Chem.*, 1982, **86**, 494; (*b*) A. Ceulemans, M. Dendooven and L. G. Vanquickenborne, *Inorg. Chem.*, 1985, **24**, 1159; (*c*) L. G. Vanquickenborne and A. Ceulemans, *Inorg. Chem.*, 1981, **20**, 796; (*d*) A. Ceulemans, personal communications.
10 (*a*) R. H. Holm, *J. Am. Chem. Soc.*, 1960, **82**, 5632; (*b*) Y. Nishida and S. Kida, *Coord. Chem. Rev.*, 1979, **21**, 275; (*c*) B. Bosnich, *J. Am. Chem. Soc.*, 1968, **90**, 627.
11 A. B. P. Lever, *Inorganic Electronic Spectroscopy*, 2nd edn., Elsevier, Amsterdam, 1984.
12 A. Böttcher, H. Elias, L. Müller and H. Paulus, *Angew. Chem., Int. Ed. Engl.*, 1992, **31**, 5.
13 S. K. Sur, *J. Magn. Reson.*, 1989, **82**, 169.
14 S. Yamada, E. Ohno, Y. Kage, A. Takeuchi, K. Yamanouche and K. Iwasaki, *Coord. Chem. Rev.*, 1968, **3**, 247.
15 A. B. P. Lever, *Coord. Chem. Rev.*, 1968, **3**, 119.
16 M. Gerloch, *Prog. Inorg. Chem.*, 1984, **31**, 371.
17 R. W. Soukup and R. Schmid, *J. Chem. Educ.*, 1985, **62**, 459.
18 (*a*) J. Becher, P. H. Olesen, N. A. Knudsen and H. Toftlund, *Sulfur Lett.*, 1986, **4**, 175; (*b*) B. S. Jensen, *Acta Chem. Scand.*, 1959, **13**, 1668; (*c*) L. Hennig and G. Mann, *Z. Chem.*, 1988, **28**, 364; (*d*) W. Dymek, B. Janik and R. P. Zimon, *Acta Pol. Pharm.*, 1963, **20**, 9 (in Polish).
19 (*a*) A. la Cour, B. Adhikhari, H. Toftlund and A. Hazell, *Inorg. Chim. Acta*, 1992, **202**, 145; (*b*) A. la Cour, M. Findeisen, C. E. Olsen, O. Simonsen and H. Toftlund, unpublished work.
20 (*a*) C. K. Johnson, ORTEP II, Report ORNL-5138, Oak Ridge National Laboratory, Oak Ridge, TN, 1976; (*b*) R. Norrestam and K. Nielsen, Technical University of Denmark, personal communication, 1982; (*c*) S. R. Hall, H. D. Flack and J. M. Stewart (Editors), *XTAL 3.2 Reference Manual*, Universities of Western Australia and Maryland, 1992; (*d*) G. M. Sheldrick, SHELXS 86, Program for the Solution of Crystal Structures, University of Göttingen, 1986; (*e*) M. S. Lehmann and F. K. Larsen, *Acta Crystallogr., Sect. A*, 1974, **30**, 580; (*f*) G. S. Pawley, in *Advances in Structure Research by Diffraction Methods*, eds. W. Hoppe and R. Mason, Pergamon, Oxford, 1971, vol. 4, pp. 1–64.

Received 28th March 1996; *Paper* 6/02209J